Published in final edited form as:
*Alcohol*. 2013 May ; 47(3): 173–179. doi:10.1016/j.alcohol.2012.12.013.

# Effects of Early Postnatal Alcohol Exposure on the Developing Retinogeniculate Projections in C57BL/6 Mice

**İlknur Dursun**[a], **Ewa Jakubowska-Doğru**[b], **Elibol-Can Birsen**[b], **Deborah van der List**[c], **Barbara Chapman**[c,d], **Lihong Qi**[e], and **Robert F. Berman**[d,f]

[a]Department of Molecular Biology and Genetics, Üsküdar University, 34662 İstanbul, Turkey

[b]Department of Biological Sciences, Middle East Technical University, 06531 Ankara, Turkey

[c]Department of Neurobiology, Physiology, and Behavior, UC Davis, Davis, CA 95616

[d]Center for Neuroscience, UCDavis, Davis, CA 95616

[e]Division of Biostatistics, Department of Public Health, Univ. California Davis, Davis, CA 95618

[f]Department of Neurological Surgery, UCDavis, Davis, CA 95616

## Abstract

Previous studies on the adverse effects of perinatal exposure to ethanol on the developing visual system mainly focused on retinal and optic nerve morphology. The aim of the present study was to investigate whether earlier reported retinal and optic nerve changes are accompanied by anomalies in eye-specific fiber segregation in the dorsal lateral geniculate nucleus (dLGN). C57BL/6 mice pups were exposed to ethanol by intragastric intubation at either 3 or 4 g/kg from postnatal days (PD) 3-10, the third trimester equivalent to human gestation. Control (C) and intubation control (IC) groups not exposed to ethanol were included. On PD9 retinogeniculate projections, were labeled by intraocular microinjections of cholera toxin-β (CTB) either conjugated to Alexa 488 (green) or 594 (red) administrated to the left and right eye, respectively. Pups were sacrificed 24 h after the last CTB injection. The results showed that ethanol exposure decreased the total number of dLGN neurons and significantly reduced the total dLGN projection as well as the contralateral and ipsilateral projection areas.

## Introduction

It is well established that perinatal exposure to ethanol has adverse effects on peripheral organs and the central nervous system. Ocular defects including microphthalmia, strabismus, increased tortuosity of the retinal vessels, hypoplasia of the optic nerve, refractive errors such as myopia, hyperopia, amblyopia and astigmatism, and/or reduced visual acuity have also been reported in about 90% of children with fetal alcohol syndrome (FAS), suggesting that ocular structures are sensitive to alcohol exposure during their development (Strömland, 1987; Strömland, 2004). Impairments in visual attention and higher visual processing have also been reported in children born to alcoholic mothers (Coles et al., 2002; Connor et al., 1999). However, the mechanisms underlying fetal alcohol-induced visual deficits are not



Corresponding Author: Robert F. Berman, Ph.D., Dept. Neurological Surgery, University of California Davis, Davis, CA 95616 USA, 530-754-5102, 530-754-5125 (fax), rfberman@ucdavis.edu.

completely clear. To better understand these mechanisms FAS animal models are used. The most common ophthalmologic defects observed in animal models of FAS, including fish (Arenzana et al., 2006; Dlugos and Rabin, 2007; Kashyap et al., 2007; Matsui et al., 2006), chick (Chmielewski et al., 1997; Tufan et al., 2007), mouse (Ashwell and Zhang, 1994; Cook et al., 1987; Kennedy and Elliott, 1986; Parson et al., 1995; Parson and Sojitra, 1995), rat (Harris et al., 2000; Philips et al., 1991; Pinazo-Duran et al., 1993, 1997; Strömland and Pinazo-Duran, 1994) and monkey (Clarren et al., 1990; Papia et al., 2010), are largely parallel to what has been observed in humans. These include microphthalmia, optic nerve hypoplasia, retinal ganglion cell loss, delayed myelination, and/or reduced myelin thickness in the optic nerve fibers.

In our previous study carried out on mouse pups exposed to ethanol during the early postnatal period between postnatal days (PD) 3-20 (Dursun et al., 2011), we found a significant reduction in the number of the retinal ganglion cells (RGCs) and alterations in the RGCs' morphology. Morphological changes included a decrease in soma size and total dendritic field area, and increase in dendrite branch angle and dendrite tortuosity. RGCs are the projection cells to the superior colliculi (SC) and dorso-lateral geniculate nuclei (dLGN). The main output from retinal ganglion cell layer goes to eye-specific regions in dLGN of thalamus which projects through the optic radiation directly to the primary visual cortex (i.e., V1, or striate cortex). In primates and humans, the lateral geniculate nucleus has several layers, and the two eyes project to separate layers (Chapman, 2003). In contrast, the lamination pattern is not obvious in rodents (De Courten and Garey, 1982; Garey and De Courten, 1983). However, appropriate experimental methods revealed a pattern of lamination referred to as "hidden lamination", with eye specific projection fields showing bilateral symmetry and the same location across animals (Discenza et al., 2008; Reese, 1988). Retrograde and anterograde labeling of the rat and mice RGC projections demonstrated that ganglion cell axons originating from nasal and most of the temporal retina (approximately 95-97% of all axon) cross at the optic chiasm (contralateral) and project to the lateral and ventral regions of the dLGN, occupying 80-85% of LGN area (Dräger and Olsen, 1980; Hayhow et al., 1962; Huberman et al., 2003; Reese, 1988; Ziburkus and Guido, 2006). The remaining 3-5% of axons originating from ventrotemporal retina represent uncrossed (ipsilateral) projections that form a core in the dorsomedial region of the dLGN, occupying 15-20% of the total LGN area (Ziburkus and Guido, 2006). In rats and mice, the ipsilateral retinogeniculate projection (up to 5% of all axons) is very small as compared with 40% of uncrossed axons in humans and is thought to be responsible for relatively poor binocular vision in these animals.

Here, it has been of interest to investigate whether a decrease in the number of RGCs and alterations in the RGCs morphology reported in mice as a result of early postnatal ethanol intoxication (Dursun et al., 2011) are accompanied by changes in the pattern of retinogeniculate projections. The expectation of ethanol adverse effect on the development and segregation of retinogeniculate projections in fetal alcohol pups arises also from the fact that in intact animals remodelling of these connections was shown to be dependent on spontaneous neural activity during perinatal development (Torborg et al., 2005; Blankenship and Feller, 2010). On the other hand it was reported that fetal ethanol causes changes in the pattern of spontaneous activity in neural circuits (Galindo and Valenzuela, 2006) and thus may have impact on remodeling of the wiring pattern during development. In mice the predominantly crossed fibers are generated on embryonic days E11-E19 and start innervating the dLGN by E 14-16. In contrast, the uncrossed fibers develop between E11-E16 and invade dLGN during the first two postnatal days. Eye specific segregation of retinogeniculate projections takes place between PD4-8 (Dräger, 1985; Godement et al., 1984; Guido, 2008a,b; Jaubert-Miazza et al., 2005; Ziburkus and Guido, 2006). Therefore, in the present study, the potential alterations in retinogeniculate projection were examined in

mice exposed to two different ethanol doses during the critical postnatal period starting from PD3 throughout PD10. Retrograde transport of Cholera toxin-β (CTB) conjugated to different fluorescent dyes was used to visualize eye-specific fiber segregation in the dorsal lateral geniculate nucleus, while quantification of the number of neurons within dLGN was done by unbiased stereological methods.

## Materials and Methods

### Subjects

Both male and female C57BL/6 mice from Charles River Laboratories (Wilmington, MA) were used in this study. Pups used in these experiments were randomly selected from different litters. All procedures were approved by the Institutional Animal Care and Use Committee of the University of California, Davis (IACUC). Animals were housed in IACUC approved animal facilities under controlled environmental conditions.

### Neonatal Treatment

The newborn pups were divided into 4 groups: nonintubated controls (C), intubation controls (IC), pups intubated with 3g/kg/body weight EtOH (A3) and pups intubated with 4g/kg/body weight EtOH (A4). The day of birth was designated as postnatal day (PD) 0. Pups in the two alcohol groups were intubated each day from PD3 to PD10 with 3g or 4g / kg body weight ethanol, respectively, delivered in a 0.02 ml / g volume of artificial enriched milk. The milk formula was prepared and kindly donated by Kelly and Lawrence (2008). The alcohol solution was divided into two equal portions given to pups two hours apart. Two hours after the second intubation, pups were reintubated with 0.02 ml/g of the milk solution alone. The pups were intubated at the same time each morning. Each day one hour before intubation, the litter was taken from the dam and placed on a heating pad maintained at 37 °C. Between intubations, the pups were returned to the dam. Intubations were carried out using PE-10 tubing (Clay Adams Brand; Becton Dickinson) lubricated with corn oil and attached to a 1-cc insulin syringe filled with milk with or without alcohol. The length of the tube was measured from the mouth to the stomach and marked. The PE-10 tube was carefully inserted down the esophagus into the stomach, and a measured amount of solution was given immediately. Pups from the IC group, a control for possible intubation-induced stress effects, were intragastrically intubated in the same manner as those from the A3 and A4 group, but received neither ethanol nor milk. The C group was not given any treatment. Pups from C groups were removed from their litter, one at a time, weighed and returned to their dams.

### Body Weight Changes

Every day prior to the first ethanol administration, all pups (C n=10, IC n=9, A3 n=12, A4 n=11) were weighed and the changes in their body weight were recorded.

### Blood Alcohol Concentration (BAC)

Blood alcohol concentration (BAC) for 2 different ethanol doses (3 and 4 g / kg / day) was measured in separate groups of pups that received the same ethanol treatment as the animals used for mapping retinogeniculate projections and stereology. Between 3 and 5 different pups were used for each PD and each time point. On PD3 and PD10 pups were anesthetized in an ice bath until movement stopped then decapitated. Blood samples were collected in a heparinized capillary tube at 1, 1.5 and 2 hour after second intubation. Blood samples were centrifuged at 10000 rpm, at 4 °C for 5 minutes (Brinkmann Instruments Inc, Westbury, NY). Plasma was taken and kept at -80 °C. BACs were analyzed using an oximetric

procedure (Helfer et al., 2009) with an Analox GL5 Alcohol Analyzer (Analox Instruments, Lunenburg, MA).

### Anterograde labeling of retinogeniculate projections and tissue collection

On PD9, pups in each group were anesthetized with a mixture containing 3.5 mg/kg ketamine and 2.1 mg/kg xylazine in 0.9% sterile sodium chloride saline solution. Borosilicate glass micropipettes (Sutter Instrument Co., Novato, CA, USA) were pulled on a Flaming/Brown micropipette puller (Sutter Instrument Co.) and filled with 1-1.5 μl cholera toxin-β (CTB) either conjugated to Alexa 488 or Alexa 594 (Invitrogen, Carlsbad, CA). The eyelids were opened and intraocular injections of CTB conjugated with Alexa 488 (green) or 594 (red) were administrated to the left and right eye, respectively. The eyes were treated with a triple antibiotic ophthalmic ointment and the animal was placed on a heating pad maintained at 37 °C until full recovery from anesthesia and then returned to the dam. On PD10, pups received the same milk-alcohol mix as on the previous day. Twenty-four hours after CTB injection mice were sacrificed with a lethal injection of (0.1ml, i.p.) Fatal Plus (Vortech Pharmaceuticals, Dearborn, MI). The brains were removed from the skull and fixed for 2 days in 4% paraformaldehyde (PFA, Sigma, St. Louis, MO) in 0.1M phosphate buffered saline (PBS, EMD Chemicals Inc. Gibbstown, NJ). Then, brains were embedded in 3.5% agar (Sigma, St. Louis, MO) and sectioned at 50 μm in the coronal plane using a vibratome (Leica Microsystems, Bannockburn, IL). Each cut section was mounted on a glass slide then cover slipped before imaging.

### Pup loss over the course of the experiments

Pup loss from the experimental procedures was unexpectedly high (i.e., 55% mortality), as detailed below. A total of 44 pups were initially used in this study, divided into four groups: Control (C, n=10), Intubated Control (IC, n=10), 3 g/kg/day Alcohol (A3, n=14) and 4 g/kg/day (A4, n=10). The final number of pups for which CTB labeling data were available was 20; with final group numbers of 5, 3, 7 and 5 for groups C, IC, A3 and A4, respectively. The attrition was due either to death during intubation procedure, or due to death during the anesthesia prior to intraocular injections of CTB or unsuccessful CTB marker injections. There was a loss of 11 pups from lethal complications from the neonatal intubations (n= 0, 2, 5 and 4 dead for groups C, IC, A3 and A4, respectively), and a total of 13 pups lost from complications of the CTB injection procedures (n=5, 5, 2 and 1 for C, IC, A3 and A4, respectively). Chi square analyses did not indicate that there were significant differences between treatment groups in the number of pups lost overall ($X^2$=0.51, df=3, p=0.92), during intubation ($X^2$=2.2, df=2, p=0.33) or due to CTB injection ($X^2$=4.67, df=3, p=0.20). Neonatal intubation coupled with intraocular CTB injection clearly results in a very high loss of animals, and future experiments will need to start with larger group sizes or find another way to reduce pup loss from repeated neonatal ethanol intubation or intraocular CTB injection.

### Imaging and morphometric measures

Images of the dLGN from pups treated with CTB were taken on a Nikon Eclipse E600 upright microscope equipped with an CCD digital camera (Hamamatsu Photonics) using a 10x objective lens. Imaging and quantification of retinogenicular projections were carried out using similar procedures to those described previously (Ballesteros, et al., 2005; Huberman, et al., 2003). Briefly, raw images of green (Alexa 488, Fig. 1A) or red (Alexa 594, Fig. 1B) fluorescently labeled retinal ganglion cell input to the dLGN were imported to Photoshop (Adobe Systems Inc., San Jose, CA). Images were converted to gray scale, and cropped to exclude the optic tract and medial intralaminar nucleus (Fig. 2). Image intensity was set to 30% above background, and pixel intensities less than 30% above background were set to black, while intensities greater than 30% above background were set to white.

The 30% above background threshold was based on previous studies (Huberman et al., 2002; Penn et al., 1998). Measurements of the area of the dLGN receiving projections from either contralateral or ipsilateral eye were done by selecting all white pixels within the image frame using Image J (Image J, NIH). Three 50 μm thick vibratome sections from the middle portion of the dLGN per animal were used for analysis.

### Cell Count in the dorsal lateral geniculate nucleus (dLGN)

An additional 24 mice were used for stereological counts of the number of neurons in the dLGN at PD10. Mice were divided into the following 4 groups (n=6/group): C, IC, A3 and A4, and treated as described above under Neonatal Treatment. Counts of neurons within dLGN at PD10 were performed for the four animal groups: At PD 10, after the completion of ethanol treatment, mice were sacrificed with lethal dose of Fatal-Plus® and perfused with 0.1M phosphate buffer (pH 7.4), followed by 4% paraformaldehyde in 0.1M sodium phosphate buffer. Brains were then immediately removed post-fixed for 1h in 4% paraformaldehyde, cryoprotected in 10% sucrose solution for 1h and in 30% sucrose solution for 24h, and then frozen in 30% sucrose for later histological analysis. Brains were then coronally sectioned at 50μm on a sliding microtome (American Optical model 860, Buffalo, NY). Tissue sections were mounted on slides, air dried and stained with Cresyl Violet. The number of neurons within the dLGN was counted in an unbiased manner using the optical fractionator probe in the StereoInvestigator software (Microbrightfield, Williston, VT). Specifically, images were captured using Nikon E600 microscope equipped with a motorized stage controller and connected to a color video camera. Counting was performed according to the rules of the unbiased stereology with the optical dissector (West *et al.*, 1991). Volume ($\mu m^3$) of the dLGN was calculated using the Cavalieri method. On each section, the dLGN was outlined under low power magnification (100 magnification), and neurons were counted under oil immersion magnification (1000 magnification). The counting frame was set at 20μm with a grid size of 100μm. The first focal plane of the dissector was placed 2 μm below the top of the section (i.e., guard height setting). Counting was then carried out through a depth of 10 μm (dissector height). Neurons were counted if their nuclei first came into focus within the dissector height (10μm), were within the dissector frame or touching the inclusion lines, and did not touch any exclusion lines. Every 2nd tissue section was counted, and the tissue thickness was measured for each counting frame, separately. Stereological analysis were carried out to a high degree of sampling stringency (coefficient of error [CE] < 0.1, shape factor m=1). The number of neurons estimated by number weighted section thickness was used for statistical analysis.

### Statistical Analyses

Group means ± SEM were calculated from all the measures. A two-way repeated measures ANOVA (day × group) was performed to evaluate the changes in body weights. The morphological data were analyzed using a one-way ANOVA, and blood-alcohol-concentrations (BAC) were analyzed using independent samples t-tests. Post hoc individual group comparisons were by post-hoc Tukey test when appropriate. Data for the areas of the total, contralateral and ipsilateral retinogeniculate projections in the dLGN were analyzed by multivariate analysis of variance (MANOVA) because data from the left and right dLGN are correlated. The Wilks's Lambda test was then used for individual group comparisons. The minimal probability level for statistical significance was set at $p<0.05$.

## Results

### Body Weight

The pups' mean body weight (± SEM) was calculated daily throughout PD3-PD10 for each group, separately (Figure 3). A two-way (treatment × day) repeated measure ANOVA

yielded only a significant increase in body weight over days for all groups [F(7,266)=889.4, p<0.0001].

### Blood Alcohol Concentration

As seen from Table 1, for both ethanol doses and both ages the peak BAC was observed 1.5 h after the second intubation. The BAC was significantly higher for the higher ethanol dose on PD3 (p=0.04) 1.5 h and on PD10 2 h after the second intubation (p=0.02). In both alcohol groups at all 3 time points, the BAC was consistently lower on PD10 compared to PD3.

### Anterograde labeling of retinogeniculate projections

In the initial statistical MANOVA all four groups were used (i.e., C, IC, A3 and A4). This analysis showed a significant treatment effect for the area of the ipsilateral projection [F(6,30)=3.15, p=0.016], while the treatment effects for contralateral and total areas did not reach statistical significance (p=0.067 and p=0.087, respectively). Individual pair-wise group comparisons showed that the A3 differed significantly from group C (p=0.048) and the A4 alcohol group (p=0.012), and the A4 group differed significantly from group IC (p=0.04).

As described above the number of subjects in the IC control group was small, and so data from the C (n=5) and IC (n=3) control groups were pooled to create a larger C+IC control group (n=8) for a second statistical analysis by MANOVA. This was justified in part by the fact that there was no statistically significance difference between the two control groups (p=0.43) and they had similar means. Data for the total, contralateral and ipsilateral dLGN projection areas from this analysis using pooled controls are shown in Figure 4. This analysis showed a significant treatment effect for Total dLGN area [F(4,32)=2.99, p=0.033]. Individual pair-wise group comparisons for Total LGN area showed that the 4g/kg/day group differed significantly from the C+IC group (p=0.05, and that the A3 group differed significantly from the A4 group (p=0.046). The C+IC group did not differ significantly from the A3 group (p=0.32). The treatment effect for the Contralateral dLGN area was also significant (F=3.52, df=4,32, p=0.017). Individual group comparisons for the Contralateral dLGN area showed that the difference between the A4 and C+IC group was significant (p=0.02), as was the difference between the A3 and A4 group (p=0.05). The difference between the C+IC group and the A3 group was not significant (p=0.48). There was also a significant treatment effect for the area of the Ipsilateral dLGN projection [F(4,32)=4.04, p=0.009]. Individual group comparisons for the Ipsilateral dLGN area showed that the A4 group differed significantly from the C+IC group (p=0.046) and that the difference between the A3 and A4 was also significant (p=0.02). The difference between the A3 and C+IC groups was not significant (p=0.18).

### Number of Neurons in the dorsal Lateral Geniculate Nucleus (dLGN)

Counts of neurons within dLGN performed at PD10 for each treatment group are presented in Fig 5. One pup each in groups C and A3 died before perfusion for histology, leaving n=5 in groups C and A3, and n=6 in groups IC and A4 for stereological analysis. ANOVA applied to evaluate these data confirmed a statistically significant alcohol treatment effect on the number of neurons in dLGN [F(3,18) = 7.19, p<0.01]. Individual post-hoc group comparisons confirmed that there were significantly fewer neurons in group A4 compared to the control group (p<0.001). No other comparisons reached statistical significance. Volumes of the dLGN did not differ significantly between treatment groups [F(3,18) = 1.32, p=0.30].

## Discussion

To our knowledge it is the first study using a rodent model of visual system development to investigate the effects of ethanol exposure during the human third trimester equivalent on eye-specific segregation of retinogeniculate projections. Two ethanol doses were examined in this study (i.e., 3 and 4 g/kg/day), but only the 4 g/kg/day dose resulted in a significant reduction in the area of the retinogeniculate projections, and this effects was seen for both the contralateral and ipsilateral projections. When applied over the relatively short period from PD3 throughout PD 10, only the higher 4 g/kg/day dose of ethanol significantly reduced the number of neurons in the dLGN as compared to controls.

As in our previous study (Dursun et al., 2011), the ethanol doses of 3 and 4 g /kg/day given in an enriched milk formula did not affect body weight gain in newborn pups. For both ethanol doses and at both ages (PD3 and PD10), the peak BAC was observed 1.5 h after the second intubation, with blood alcohol levels significantly higher for the higher ethanol dose and at the younger age. In present study, the mean BAC ranged between 256 – 577 mg/dl and was above blood alcohol levels that were earlier reported to cause alterations in the structure of the developing retina. This includes a decrease in the numbers of RGCs, changes in RGC morphology (Dursun et al., 2011; Tenkova et al., 2003), as well as malformations of the optic nerve (Harris et al., 2000; Parson et al., 1995). The decline in BAC observed in the present study in both ethanol groups with age is likely related to an increase in metabolic tolerance to alcohol along with liver maturation and an increase in the efficacy of liver alcohol detoxification system including alcohol dehydrogenase and the microsomal ethanol oxidizing enzymes (Bhalla et al., 2005; Krasner et al., 1974, Lad et al.,). The fact that the differences in BACs between the two alcohol groups were much larger at PD3 than at PD10 also supports the idea that liver capability to handle higher ethanol doses increases with age.

The present results show that in mice, binge-like ethanol exposure at 4 g/kg/day, but not 3 g/kg/day during the early postnatal period from PD3-10 significantly decreased the number of neurons in dLGN. In our earlier study (Dursun et al., 2011) a significant decrease in the count of dLGN neurons was noted also at an ethanol dose of 3 g/kg/day. However, in the former study, ethanol was administered over PDs 3-20, a much longer exposure duration than that used in the present study. A decrease in the number of dLGN neurons observed here after the early postnatal ethanol intoxication is consistent with a report by Tenkova et al., 2003, who demonstrated that neurons in the dLGN, superior colliculus, and visual cortex were highly susceptible to ethanol's apoptogenic action especially on postnatal days PD4 to PD7.

One of the important means to evaluate the effects of adverse events such as visual deprivation or drug intoxication on visual system development is the investigation of ocular dominance plasticity. In the present study, to examine the potential changes in the development of ocular dominance, the immunohistochemical anterograde labeling of retinal output neurons was performed in both control and ethanol exposed mice pups at PD10, a day by which the eye-specific segregation of retinogeniculate projection is completed in this species (Godement et al., 1984; Guido, 2008; Jaubert-Miazza et al., 2005). The analysis of retinogeniculate projections in control and ethanol exposed mice pups confirmed that the contralateral projection is highly dominant occupying approximately 85% of the total area in LGN. This result was expected and confirms that the anterograde labeling of retinogeniculate fibers and estimation of the segregation of inputs from the two eyes in the present study were successful and the results consistent with previous reports (Dräger and Olsen, 1980; Ziburkus and Guido, 2006). In the current study the separate analysis of contra- and ipsilateral retinogeniculate projections shows that the effects of early postnatal ethanol

intoxication were found in both the contralateral and ipsilateral projections. It is likely that alcohol effects on the contralateral projections would have more serious consequences for vision. However, although the ipsilateral projection represents only approximately 15% of the total retinogenicuate projection, alcohol effects may still be affect vision. Interestingly, Drager and her associates (Balkema and Dräger, 1990; Dräger and Olsen, 1980) examined the origins of ipsilateral and contralateral retinal projections in pigmented and albino mice and postulated that one of the reasons for poor vision in albino mice, compared to the pigmented mice, might be an overall reduction in ipsilaterally projecting cells in albinos. Despite its smaller morphological representation in dLGN compared to the contralateral projection, the ipsilateral retinofugal projections in small rodents still represents between 30–60 deg of frontal visual space. There is also a large discrepancy between the ratio of contralateral-to-ipsilateral representation in retina and the strength of physiological responses of each eye in dLGN and the primary visual cortex (V1) (Sefton et al., 2004). Specifically, a stimulus from a binocular segment of visual field activates 9 times more RGCs in the contralateral retina as in the ipsilateral retina (Coleman et al., 2009). However, at the level of dLGN, the proportion of contra to ipsilateral activation by binocular segments is only three-to-one, and this decreases further to 2:1 in visual cortex, indicating a strong convergence of both ipsilateral and contralateral at higher levels of processing of visual input. In small rodents, there is also a possibility of “cross-over” between the binocular projections at the level of dLGN where 63% of cells receiving ipsilateral input were reported to show strong excitatory responses to the stimulation of both eyes. This suggests the existence of some binocular integration at a stage earlier than previously described for the higher mammals where this type of binocular responses is first seen in the cerebral cortex (Grieve, 2005). All this factors may increase the impact of alcohol exposure on ipsilateral retino-geniculate projections and subsequently on binocular vision in rats and mice. Indeed, similar effects on retinogeniculate projections induced by fetal ethanol in human could also have much greater impact on visual functions, especially ocular dominance and binocular stereoscopic vision, than previously thought.

In conclusion, the present results demonstrate that alcohol exposure during the early postnatal period can affect eye field-specific segregation of the retinogeniculate projections, providing new information on how the visual system is impacted by alcohol during development. Interference with segregation of these visual system projections could also contribute to poor binocular vision seen in some children with fetal alcohol syndrome (Stromland and Hellstrom, 2006). The frequent involvement of the ocular system in fetal alcohol syndrome points to the importance of ophthalmologic evaluation of children with FAS.

## Acknowledgments

We thank Dr. Charles R. Goodlett for his assistance in assessment of the blood alcohol concentrations and Dr. Sandra J Kelly for the help with the liquid diet formulation. We also thank Dr. Jurgen Wenzel for his guidance on histology. A portion of this work was completed in the laboratory of Dr. Leo M. Chalupa in the Department of Neurobiology, Physiology and Behavior, College of Biological Science, UC Davis. This research was supported by grants from the National Eye Institute of the NIH EY003991 and P30EY12576 to Dr. Leo M. Chalupa and partially by the METU research fund BAP-08-11-DPT-2002-K120510 through a METU–UCDavis collaboration.

## References

Arenzana FJ, Carvan MJ, Aijón J, Sánchez-González R, Arévalo R, Porteros A. Teratogenic effects of ethanol exposure on zebrafish visual system development. Neurotox Teratol. 2006; 28:342–348.

Ashwell KW, Zhang LL. Optic nerve hypoplasia in an acute exposure model of the Fetal Alcohol Syndrome. Neurotoxicol Teratol. 1994; 16:161–167. [PubMed: 8052190]

Balkema GW, Dräger UC. Origins of uncrossed retinofugal projections in normal and hypopigmented mice. J Vis Neurosci. 1990; 4:595–604.

Ballesteros JM, Van der List DA, Chalupa LM. Formation of eye-specific retinogeniculate projections occurs prior to the innervation of the dorsal lateral geniculate nucleus by cholinergic fibers. Thalamus Relat Syst. 2005; 3:157–163. [PubMed: 19367340]

Bhalla S, Kaur K, Mahmood A, Mahmood S. Postnatal development of alcohol dehydrogenase in liver & intestine of rats exposed to ethanol in utero. Indian J Med Res. 2005; 121:39–45. [PubMed: 15713978]

Blankenship AG, Feller MB. Mechanisms underlying spontaneous patterned activity in developing neural circuits. Nat Rev Neurosci. 2010; 11(1):18–29. [PubMed: 19953103]

Chapman, B. The Development of Eye-Specific Segregation in the Retino-Geniculo-Striate Pathway. In: Chalupa, LM.; Werner, JS., editors. The Visual Neurosciences. Vol. I. MIT Press; Cambridge, MA, USA: 2003. p. 108-116.

Chmielewski CE, Hernandez LM, Quesada A, Pozas JA, Picabea L, Prada FA. Effects of ethanol on the inner layers of chick retina during development. Alcohol. 1997; 14:313–317. [PubMed: 9209545]

Clarren SK, Alvord EC Jr, Sumi SM, Streissguth AP, Smith DW. Brain malformations related to prenatal exposure to ethanol. J Pediatr. 1978; 92:64–67. [PubMed: 619080]

Coleman JE, Law K, Bear MF. Anatomical origins of ocular dominance in mouse primary visual cortex. Neuroscience. 2009; 161:561–571. [PubMed: 19327388]

Coles CD, Platzman KA, Lynch ME, Freides D. Auditory and visual sustained attention in adolescents prenatally exposed to alcohol. Alcohol Clin Exp Res. 2002; 26:263–271. [PubMed: 11964567]

Connor PD, Streissguth AP, Sampson PD, Bookstein FL, Barr HM. Individual differences in auditory and visual attention among fetal alcohol-affected adults. Alcohol Clin Exp Res. 1999; 23:1395–1402. [PubMed: 10470983]

Cook CS, Nowotny AZ, Sulik KK. Fetal alcohol syndrome. Eye malformations in a mouse model. Arch Ophthalmol. 1987; 105:1576–1581. [PubMed: 3675291]

De Courten C, Garey LJ. Morphology of the neurons in the human lateral geniculate nucleus and their normal development. A Golgi study Exp Brain Res. 1982; 47:159–171.

Discenza CB, Karten HJ, Reinagel P. Anatomical targets of retinal ganglion cell axons in the Long-Evans rat. 2008 SFN 2008 458.3 EE16.

Dlugos CA, Rabin RA. Ocular deficits associated with alcohol exposure during zebrafish development. J Comp Neurol. 2007; 502:497–506. [PubMed: 17394139]

Dräger UC, Olsen JF. Origins of crossed and uncrossed retinal projections in pigmented and albino mice. J Comp Neurol. 1980; 191:383–412. [PubMed: 7410600]

Dräger UC. Birth dates of retinal ganglion cells giving rise to the crossed and uncrossed optic projections in the mouse. Proc R Soc Lond B Biol Sci. 1985; 224:57–77. [PubMed: 2581263]

Dursun I, Jakubowska-Dogru E, van der List D, Liets LC, Coombs JL, Berman RF. Effects of Early Postnatal Exposure to Ethanol on Retinal Ganglion Cell Morphology and Numbers of Neurons in the Dorsolateral Geniculate in Mice. Alcohol Clin Exp Res. 2011; 35:2063–2074. [PubMed: 21651582]

Frenkel MY, Bear MF. How monocular deprivation shifts ocular dominance in visual cortex of young mice. Neuron. 2004; 44:917–923. [PubMed: 15603735]

Galindo R, Valenzuela CF. Immature hippocampal neuronal networks do not develop tolerance to the excitatory actions of ethanol. Alcohol. 2006; 40:111–118. [PubMed: 17307647]

Garey LJ, de Courten C. Structural development of the lateral geniculate nucleus and visual cortex in monkey and man. Behav Brain Res. 1983; 10:3–13. [PubMed: 6639728]

Godement P, Salaün J, Imbert M. Prenatal and postnatal development of retinogeniculate and retinocollicular projections in the mouse. J Comp Neurol. 1984; 230:552–575. [PubMed: 6520251]

Grieve KL. Binocular visual responses in cells of the rat dLGN. J Physiol. 2005; 566:119–124. [PubMed: 15905208]

Guido W. Refinement of the retinogeniculate pathway. J Physiol. 2008a; 586:4357–4362. [PubMed: 18556365]

Guido, W. Development of the Retinogeniculate Pathway. In: Chalupa, LM.; Williams, RW., editors. Eye, Retina, and Visual System of The Mouse. The MIT press; Cambridge, Massachusetts London, England: 2008b. p. 415-427.

Hayhow WR, Sefton A, Webb C. Primary optic centers of the rat in relation to the terminal distribution of the crossed and uncrossed optic nerve fibers. J Comp Neurol. 1962; 118:295–321. [PubMed: 13905663]

Harris SJ, Wilce P, Bedi KS. Exposure of rats to a high but not low dose of ethanol during early postnatal life increases the rate of loss of optic nerve axons and decreases the rate of myelination. J Anat. 2000; 197:477–485. [PubMed: 11117631]

Helfer JL, Calizo LH, Dong WK, Goodlett CR, Greenough WT, Klintsova AY. Binge-like postnatal alcohol exposure triggers cortical gliogenesis in adolescent rats. J Comp Neurol. 2009; 514:259–271. [PubMed: 19296475]

Huberman A, Stellwagen D, Chapman B. Decoupling eye-specific segregation from lamination in the lateral geniculate nucleus. J Neurosci. 2002; 22:9419–9429. [PubMed: 12417667]

Huberman A, Wang GY, Liets LC, Collins OA, Chapman B, Chalupa LM. Eye-specific retinogeniculate segregation independent of normal neuronal activity. Science. 2003; 300:994–998. [PubMed: 12738869]

Hughes A. The refractive state of the rat eye. Vision Res. 1977; 17:927–939. [PubMed: 595399]

Jaubert-Miazza L, Green E, Lo FS, Bui K, Mills J, Guido W. Structural and functional composition of the developing retinogeniculate pathway in the mouse. Visual Neurosci. 2005; 22:661–676.

Kashyap B, Frederickson LC, Stenkamp DL. Mechanisms for persistent microphthalmia following ethanol exposure during retinal neurogenesis in zebrafish embryos. Visual Neurosci. 2007; 24:409–421.

Kelly SJ, Lawrence CR. Intragastric intubation of alcohol during the perinatal period. Methods Mol Biol. 2008; 447:101–110. [PubMed: 18369914]

Kennedy LA, Elliott MJ. Ocular changes in the mouse embryo following acute maternal ethanol intoxication. Int J Develop Neurosci. 1986; 4:311–317.

Krasner J, Eriksson M, Yaffe SJ. Developmental changes in mouse liver alcohol dehydrogenase. Biochem Pharmacol. 1974; 23:519–522. [PubMed: 4822739]

Lad PJ, Shoemaker WJ, Leffert HL. Developmental changes in rat liver alcohol dehydrogenase. Dev Biol. 1984; 105(2):526–529. [PubMed: 6383901]

Matsui JI, Egana AL, Sponholtz TR, Adolph AR, Dowling JE. Effects of ethanol on photoreceptors and visual function in developing zebrafish. Invest Opth Vis Sci. 2006; 47:4589–4597.

Papia MF, Burke MW, Zangenehpour S, Palmour RM, Ervin FR, Ptito M. Reduced soma size of the M-neurons in the lateral geniculate nucleus following foetal alcohol exposure in non-human primates. Exp Brain Res. 2010; 205:263–271. [PubMed: 20661554]

Parson SH, Dhillon B, Findlater GS, Kaufman MH. Optic nerve hypoplasia in the fetal alcohol syndrome: a mouse model. J Anat. 1995; 186:313–320. [PubMed: 7649829]

Parson SH, Sojitra NM. Loss of myelinated axons is specific to the central nervous system in a mouse model of the fetal alcohol syndrome. J Anat. 1995; 187:739–748. [PubMed: 8586571]

Penn AA, Riquelme PA, Feller MB, Shatz CJ. Competition in retinogeniculate patterning driven by spontaneous activity. Science. 1998; 279:2108–2112. [PubMed: 9516112]

Phillips DE, Krueger SK, Rydquist JE. Short-and long-term effects of combined pre-and postnatal ethanol exposure (three trimester equivalency) on the development of myelin and axons in rat optic nerve. Int J Develop Neurosci. 1991; 9:631–647.

Pinazo-Duran MD, Renau-Piqueras J, Guerri C. Developmental changes in the optic nerve related to ethanol consumption in pregnant rats: Analysis of the ethanol-exposed optic nerve. Teratology. 1993; 48:305–322. [PubMed: 8278930]

Pinazo-Duran MD, Renau-Piqueras J, Guerri C, Strömland K. Optic nerve hypoplasia in fetal alcohol syndrome: an update. Eur J Ophthal. 1997; 7:262–270. [PubMed: 9352281]

Reese BE. Hidden lamination' in the dorsal lateral geniculate nucleus: the functional organization of this thalamic region in the rat. Brain Res. 1988; 472:119–137. [PubMed: 3289687]

Sefton, SJ.; Dreher, B.; Harvey, A. Visual system. In: Paxinos, G., editor. The Rat Nervous System. Academic Press; Burlington, MA, USA: 2004. p. 1083-1141.

Strömland K. Ocular involvement in the fetal alcohol syndrome. Surv Ophthal. 1987; 31:277–284.

Strömland K, Pinoza-Duran MD. Optic nerve hypoplasia: Comparative effects in children and rats exposed to alcohol during pregnancy. Teratology. 1994; 50:100–111. [PubMed: 7801297]

Stromland K. Visual impairment and ocular abnormalities in children with fetal alcohol syndrome. Addict Biol. 2004; 9(2):153–157. [PubMed: 15223541]

Stromland K, Hellstrom A. Fetal alcohol syndrome – an ophthalmological and socioeducational prospective study. Pediatrics. 2006; 6(1):845–850.

Tenkova T, Young C, Dikranian K, Labruyere J, Olney JW. Ethanol induced apoptosis in the developing visual system during synaptogenensis. Invest Opth Vis Sci. 2003; 44:2809–2817.

Torborg CL, Hansen KA, Feller MB. High frequency, synchronized bursting drives eye-specific segregation of retinogeniculate projections. Nat Neurosci. 2005; 8:72–78. [PubMed: 15608630]

Tufan AC, Abbana C, Akdogan I, Erdogan D, Ozogul C. The effect of in ovo ethanol exposure on retina and optic nerve in a chick embryo model system. Rep Toxicol. 2007; 23:75–82.

Wiesenfeld Z, Branchek T. Refractive state and visual acuity in the hooded rat. Vision Res. 1976; 16:823–827. [PubMed: 960609]

Ziburkus J, Guido W. Loss of binocular responses and reduced retinal convergence during the period of retinogeniculate axon segregation. J Neurophysiol. 2006; 96:2775–2784. [PubMed: 16899631]

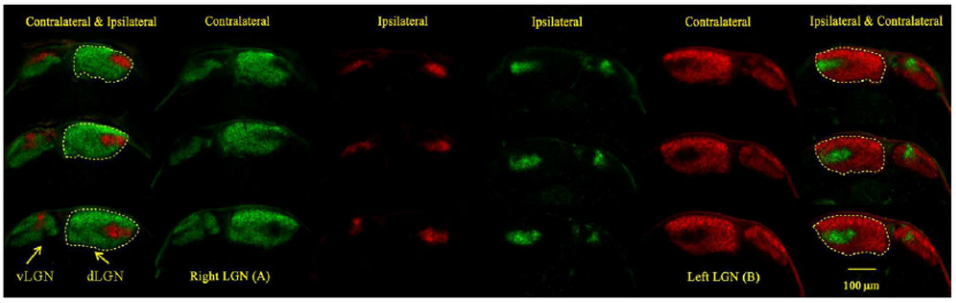


**Fig. 1.**

Visualization of retinogeniculate afferents in control mice at P10 showing the merged representations of contralateral and ipsilateral retinal inputs to the LGN. Axons from the left eye are shown in green (A). Axons from the right eye are shown in red (B). Dashed yellow lines indicate boundaries of the dLGN. Scale bar: 100 μm

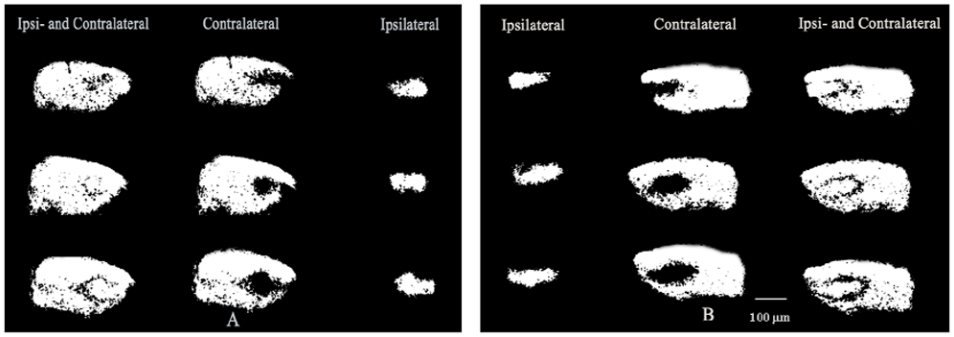


**Fig. 2.**

Gray scaled images of eye specific retinogeniculate projections in control mice at P10. A: the left eye projections and B: the right eye projections. Scale bar: 100 μm

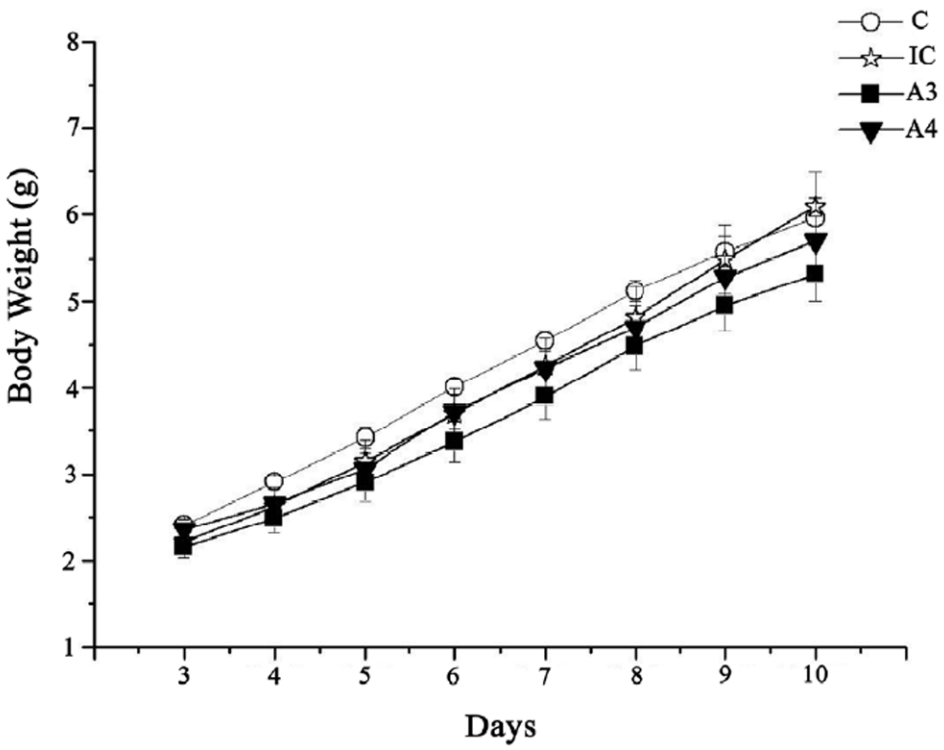


**Fig. 3.**
Body weight gain across postnatal days (PD) 3–10 for all treatment groups.

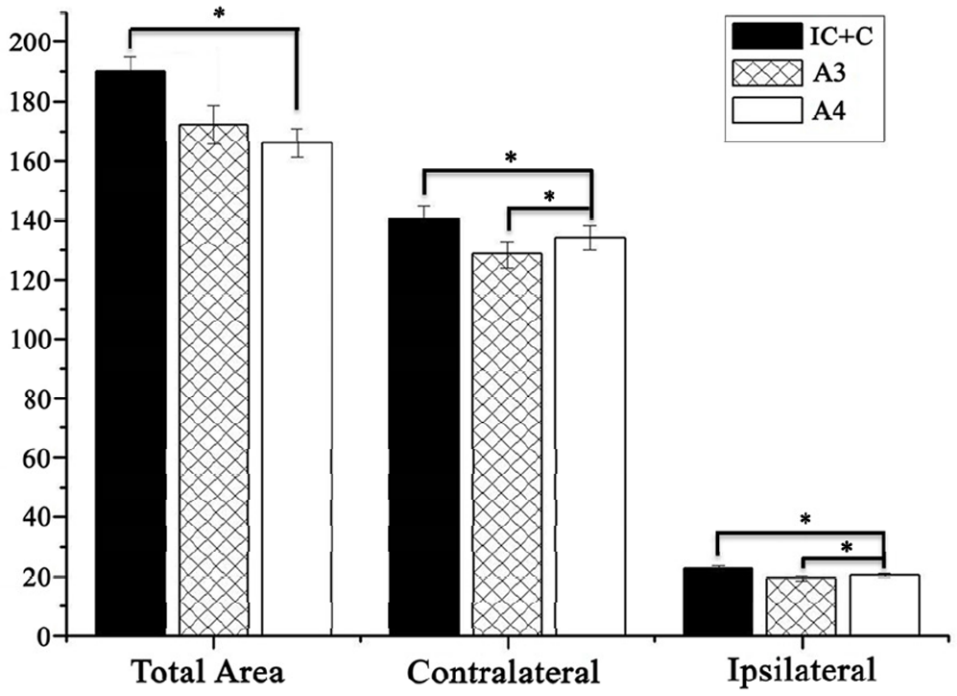


**Fig 4.**

The total dLGN projection area (Total Area) and the areas occupied by contra and ipsilateral retinogeniculate projections at P10 in IC+C, A3, and A4 groups, respectively. All areas are presented as pixel intensity ($\times 10^3$). Errors bars denote SEM. *P<0.05.

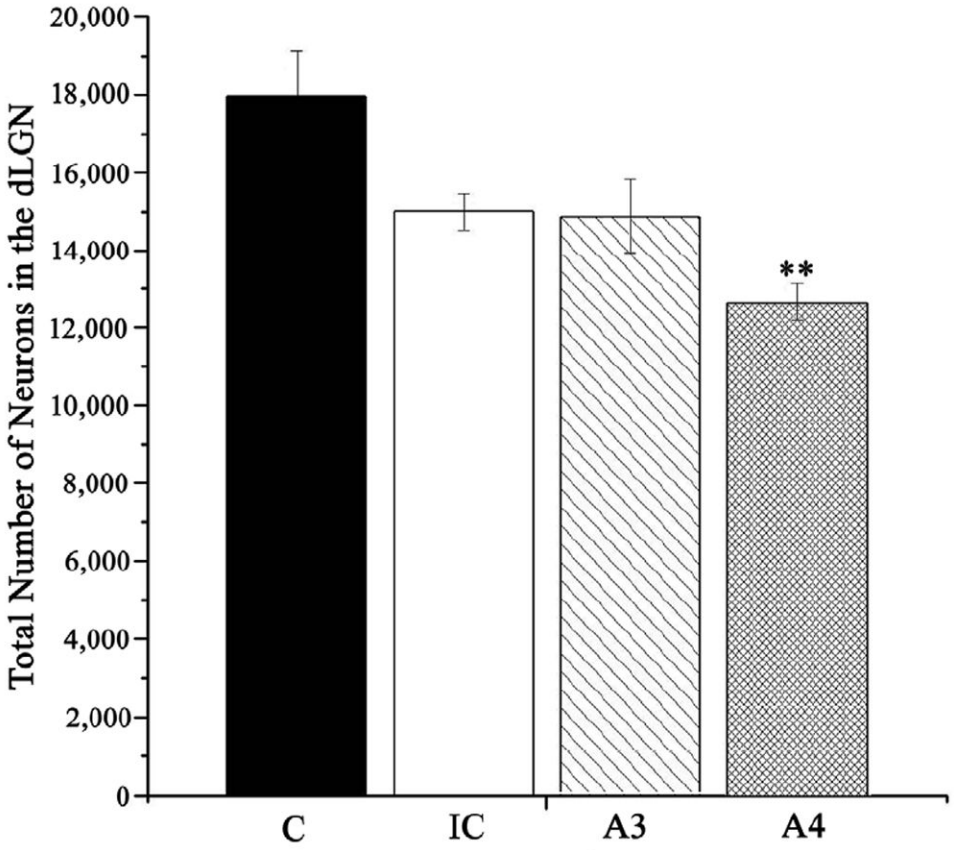


**Fig. 5.**
Number of neurons in the dLGN estimated at P10 for all treatment groups. Error bars denote SEM. **p<0.001 compared to the control group (group C).

## Table 1

Blood Alcohol Concentrations (mg/dl)[1]

| | | Time points | | |
|---|---|---|---|---|
| **Dosage** | **Age** | **1h** | **1.5h** | **2h** |
| 3g/kg EtoH | PD 3 | 265 ± 9.6 | 298 ± 5.9 | 248 ± 3.6 |
| | PD 10 | 248 ± 8.5 | 256 ± 22.7 | 201 ± 4.9 |
| 4/kg EtoH | PD 3 | 307 ± 21.8 | 492 ± 42.8 | 320 ± 33.4 |
| | PD 10 | 243 ± 38.8 | 288 ± 15.9 | 256 ± 13.3 |

[1]Values represent the mean ± standard error of the mean (S.E.M)